Atomistic simulations of the nanometer-scale indentation of amorphous-carbon thin films

S. B. Sinnott[a)]
Department of Chemical and Materials Engineering, The University of Kentucky, Lexington, Kentucky 40506-0046

R. J. Colton and C. T. White
Chemistry Division, Naval Research Laboratory, Washington, DC 20375-5342

O. A. Shenderova and D. W. Brenner
Department of Materials Science and Engineering, North Carolina State University, Raleigh, North Carolina 27695

J. A. Harrison
Chemistry Department, United States Naval Academy, Annapolis, Maryland 21402

(Received 24 October 1996; accepted 17 February 1997)

Molecular dynamics simulations are used to examine the nanometer-scale indentation of a thin film of amorphous carbon with a nonrigid sp^3 bonded carbon tip. The simulations show in detail the atomic-scale mechanism of the indentation process and compare the bonding character of the film before and after indentation. The computationally determined elastic modulus of the amorphous-carbon film is found to be 243 GPa, in good agreement with experiment. © *1997 American Vacuum Society.* [S0734-2101(97)07303-X]

I. INTRODUCTION

Rapid advances in proximal probe technology over the last decade have changed our ability to investigate, process, and manipulate materials at the nanometer scale, where their properties are no longer similar to the bulk.[1] As this important new realm of nanometer-scale materials engineering continues to be explored and understood, our ability to manufacture new devices will grow.

One widely used proximal probe is the atomic force microscope (AFM),[2,3] which is used to study nanometer-scale mechanical and surface properties of materials.[4–13] These experiments have motivated these simulations, where the nanometer-scale indentation of a hydrogen-terminated, amorphous-carbon (a-C:H) thin film is investigated with molecular dynamics (MD) simulations. There have been several other simulations of tip-surface interactions,[14–17] including the indentation of amorphous carbon with an earlier version of the hydrocarbon potential employed here, using a diamond tip that was held rigid throughout the indentation.[17]

The goals of the current work are threefold: (1) to determine the atomic-scale mechanisms of nanometer-scale indentation, (2) to examine bonding and stress distribution changes in a-C:H thin films as a result of indentation, and (3) to compare the computationally determined Young's modulus of a-C:H to experimental results. This simulation uses an improved version[18] of a widely used hydrocarbon potential originally developed by Brenner.[19] The resulting atomic-scale picture of the indentation process should provide valuable insight into experiments involving mechanical testing using atomic force microscopes and nanoindentation instruments.

a)Electronic mail: sinnott@engr.uky.edu

II. METHODOLOGY

The MD simulations are performed by integrating Newton's equations of motion with a third-order Nordsieck predictor corrector using a time step of 0.2 fs.[20] The forces on the individual atoms are derived from a reactive-empirical bond-order (REBO) hydrocarbon potential that accurately reflects the energetics, bond lengths, and lattice constants of both solid-state (diamond and graphite) and gas-phase hydrocarbon materials.[19] However, it yielded elastic constants which were generally lower than experimental values.[15–17] Hence, this potential has been modified (improved) to accurately reproduce the elastic constants of diamond and graphite while maintaining its original properties. The improved potential yields elastic constants for diamond of $c_{11}=10.78\times10^{11}$ N m^{-2}, $c_{12}=1.31\times10^{11}$ N m^{-2}, and $c_{44}=6.8\times10^{11}$ N m^{-2}, which are in good agreement with the experimental values of $c_{11}=10.76\times10^{11}$ N m^{-2}, $c_{12}=1.25\times10^{11}$ N m^{-2}, and $c_{44}=5.8\times10^{11}$ N m^{-2}.[21] The elastic constants are obtained from calculated dispersion curves[22] (frequency versus reduced wave vector). The potential is not explicitly fit to experimental data for amorphous carbon; hence, its characterization of amorphous carbon in the simulations is purely predictive.

The improved REBO potential includes improved analytic functions for the intramolecular interactions and an expanded fitting database, which includes molecular-bond energies, barriers for the formation of various radicals, and vibrational frequencies and heats of formation of many organic molecules. The electrons are not treated explicitly, however, so forces arising from effects such as orbital resonances and symmetry are not realistically treated. Furthermore, the potential is relatively short ranged, so long-range van der Waals or related forces are neglected. Recently, the im-

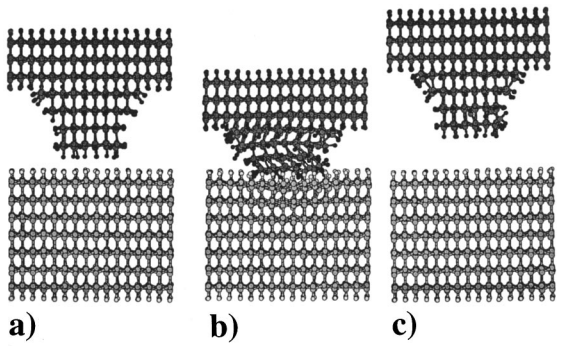

FIG. 1. Snapshots from a simulation where a diamond (111) surface is indented by a sp^3 bonded tip. The dark gray spheres are the carbon atoms in the tip, the light gray spheres are the carbon atoms in the surface, the white spheres represent surface hydrogen atoms, and the black spheres represent tip hydrogen atoms. (a) Time=0.0 ps, (b) time=6.0 ps, (c) time=15.0 ps.

proved REBO potential was used successfully to simulate the selective patterning of diamond surfaces.[23]

The tip used in the indentation simulation is a flat-ended, sp^3 bonded carbon tip. The test specimens are a hydrogen-terminated diamond (111) substrate (C(111):H) and a hydrogen-terminated *a*-C:H film on a diamond (111) surface. The C(111):H substrate is composed of 14 layers of carbon with each layer containing 64 atoms. The bottom and top layers are hydrogen terminated with 64 atoms. Thus, the C(111):H substrate contains 1024 total atoms [Fig. 1(a)]. The tip is constructed by removing atoms from (111) diamond so that a structure with low surface stress resembling an inverted pyramid with a flattened apex is formed [Fig. 1(a)]. Hydrogen atoms are added to meet the valence requirements of carbon. The tip contains 696 total atoms, 197 in the pyramidal asperity and 499 atoms in the base to which the asperity is attached. (For the *a*-C:H simulations the base of the tip contains 1176 atoms so that it will match the periodic boundary conditions of the larger *a*-C:H system.) The projected contact radius of the flat-ended apex is estimated to be about 6 Å.

The *a*-C:H system is composed of diamond (111) covered by amorphous carbon. The diamond substrate consists of six layers of carbon with each layer composed of 166 atoms. The carbon layer furthest from the tip and the surface are hydrogen terminated. The *a*-C:H film contains 2672 carbon atoms, while the total number of atoms in the substrate [film+diamond (111)] is 4000 [Fig. 3(a)]. Thus, the total number of atoms (tip and substrate) in the amorphous-carbon film simulation is 5373.

The *a*-C:H film is produced by heating the center 20 layers of a three-dimensional 60 layer slab of diamond to 8000 K while holding the remaining atoms fixed in the ideal diamond lattice structure. The heated section is allowed to disorder completely, and then quenched to room temperature at a rate of 7.7 K/fs. After equilibrating the system at 300 K, all the rigid carbon atoms on one side of the disordered region are removed and replaced by terminating hydrogen atoms to create the *a*-C:H film. The rigid carbon atoms on the other side are allowed to relax; the six layers nearest the amorphous region comprise the diamond substrate in the indentation simulation. Prior to indentation, about 21% of the carbon atoms in the film are sp^3 hybridized, 58% are sp^2 hybridized, less than 2% have two nearest neighbors, and about 0.1% have five nearest neighbors. The remaining atoms are at the film edges. Experimentally, amorphous carbon produced by evaporation or sputtering of graphite is mainly sp^2 hybridized, while amorphous-carbon films obtained by mass-selected ion beam deposition are primarily sp^3 hybridized, although there is some dependance in each case on the exact deposition conditions including the percent of atomic hydrogen incorporated into the film. Simulations with the earlier version of the potential created amorphous-carbon films through molecular deposition that were 10%–16% sp^2-like depending on deposition energy.[24]

Experimentally, *a*-C:H films contain residual stresses.[25,26] The magnitude of the residual stress depends on many variables, among them deposition conditions, substrate identity, film thickness, and sp^2 to sp^3 ratio. A stress analysis of the *a*-C:H film in our simulation shows a random distribution of internal compressive and shear (von Mises) stresses, where about 2% of the atoms have shear (6% have compressive) stresses in excess of 64 GPa. The average compressive stress in the film is about 4.0 GPa while the average shear (von Mises) stress is about 2.5 GPa. Experimentally, stresses in amorphous carbon depend on the substrate on which the film is grown and the deposition conditions; average total values ranging from 0.8 to 2.5 GPa have been reported.[27]

Starting configurations for the simulations are shown in Figs. 1(a) and 3(a). The two outermost layers of the tip and the substrate are held rigid. Moving towards the center of each figure, a Langevin thermostat is applied to the next two layers within the substrate (three layers within the substrate for the *a*-C:H film), and the next two layers within the tip to control the temperature of the system.[28] The remaining atoms evolve in time according to Newton's equations of motion with no constraints. Both tip-substrate systems are fully equilibrated at 300 K prior to indentation. To simulate an infinite surface, periodic boundary conditions are applied in the plane perpendicular to the indentation direction.

Indentation of both systems is performed by moving the rigid layers of the tip 0.05 Å closer to the substrate and equilibrating for 400 time steps. This process is repeated to achieve indentation, thus insuring that the temperature of the system remains close to 300 K. Retraction of the tip is performed by moving the rigid layers away from the substrate at the same rate and equilibrating. The force on the tip is taken to be the sum of the forces on the rigid-layer tip atoms averaged over the last 100 steps of the 400 step equilibration to minimize fluctuations in the force due to the relaxation of atoms between movements of the tip.

III. RESULTS AND DISCUSSION

A. C(111):H substrate

Simulations of the indentation of C(111):H were done to assess the mechanical properties of the tip, which are as-

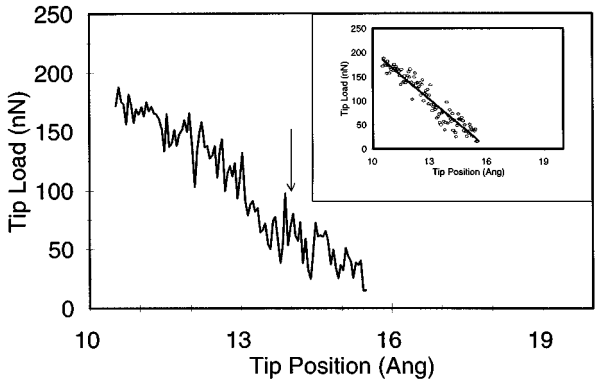

FIG. 2. Force on the tip vs distance of the tip for the indentation of the diamond (111) surface. Only the loading portion of the curve is shown. The arrow indicates the point where the tip first touches the surface. The inset shows the line of best fit to the data.

sumed to be softer than bulk diamond. Pictures of a typical indentation of C(111):H are shown in Figs. 1(a)–1(c) as a function of time. While the data from only one indentation simulation are shown, additional simulations where the tip interacts with a different part of the surface show similar results. These results are used to ascertain the nature of the tip-surface interaction. For example, comparing the pictures before and after indentation [Figs. 1(a) and 1(c)] shows a lack of adhesion and permanent deformation. Therefore, this interaction under the present loading conditions is considered elastic. Figure 2 shows the load on the tip as it pushes against the diamond surface as a function of the distance that the tip travels. The arrow indicates the point where the tip comes into physical contact with the surface. Thus, in this simulation, the tip deforms by about 4 Å.

Simulated force-distance curves can be used to calculate the reduced elastic modulus of the tip-sample system. For an elastic indent, the slope of the loading portion of the force curve is related to the reduced modulus. The relationship varies depending on the geometry of the indentor. For example, classical elasticity theory predicts a linear relationship for flat-ended indentors and a nonlinear relationship for spherical or conical indentors. Force-distance curves obtained with nominally pointed AFM indentors are usually linear.[6]

For the C(111):H substrate, the force-distance curve in the loading region is linear. Therefore, the relationship relating the slope to reduced elastic modulus is given by[29]

$$F = 2E_r a h, \tag{1}$$

where F is the force, E_r is the reduced elastic modulus, a is the radius of the contact area, and h is the penetration depth. The reduced modulus is given by

$$1/E_r = (1-\nu_1^2)/E_1 + (1-\nu_2^2)/E_2, \tag{2}$$

where ν is Poisson's ratio and subscripts 1 and 2 denote tip and substrate, respectively.

The slope $(\Delta F/\Delta h)$ of the loading portion of the force-distance curve shown in Fig. 2 (inset) obtained by linear regression[30] is 33.5 nN/Å. Using a projected radius of contact of 6.0 Å, Eq. (1) yields a reduced modulus of 279 GPa. (It is worth noting that the value of the reduced modulus depends on the value used for the contact area of the tip. Recent simulations have shown that for covalent materials the geometry of the indentation in the plane of the surface is not the physical geometry of the indentor.[31] Thus, it is difficult to determine an accurate radius of contact. For this reason, the same indentor is used for all the indentations discussed here.)

It is clear from an analysis of the atomic positions as a function of time [Figs. 1(a)–1(c)] that the tip deformation includes significant twist and shear components during the indentation while the diamond (111) substrate undergoes only slight deformation. It is suspected that these deformation mechanisms are due to the shape of the tip (with no extensive, stabilizing lattice) and the hydrogen–hydrogen repulsion between the tip and the substrate. This would account for the tip being significantly softer than the diamond (111) substrate.

The Young's modulus of diamond (111), $E(111)$, can be calculated from elastic constants, c_{ij}, derived from the REBO potential using[32]

$$E(111) = \frac{6c_{44}(c_{11}+2c_{12})}{(c_{11}+2c_{12}+4c_{44})}. \tag{3}$$

Equation (3) yields a value of about 1347 GPa. Using Eq. (2),[33] the elastic modulus of the tip is 357 GPa. Although the tip was expected to be softer than bulk diamond, it is still surprising to note the order of magnitude difference in modulus. This much smaller modulus accounts for the lack of any significant penetration of the diamond surface by this tip. One can conclude from this result that other sp^3 bonded carbon structures that are small enough to lack an extensive lattice network have mechanical properties that are also significantly different from bulk diamond. This result may be applicable to understanding the properties of diamond asperities encountered in processes such as tribology.

B. *a*-C:H film

The same tip is used to indent the *a*-C:H film. As the indentation proceeds [Figs. 3(a)–3(c)], the tip penetrates the surface of the thin film and only deforms slightly via shear, in contrast to the case for the diamond (111) surface. The tip penetrates about 4.0 Å, which is about 20% of the total thickness of the film. In a uniform film, one would expect a classical distribution of compressive stresses at the end of the tip, with shear (von Mises) stresses at the edges. However, an analysis of the stress distributions in the *a*-C:H film at the point of maximum indent indicates that atoms in the film compress in a nonuniform manner at the end of the tip, forming a jagged pattern of compression, rather than the expected parabolic distribution. This is probably due to the fact that amorphous carbon can be thought of as carbon clusters with

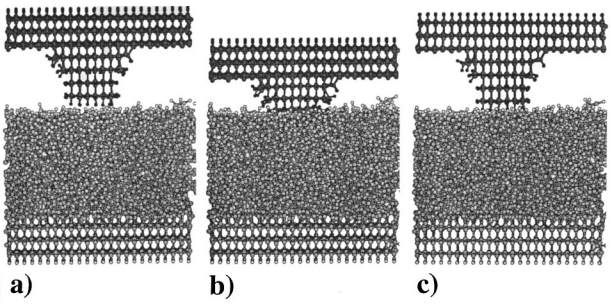

FIG. 3. Snapshots from a simulation where an amorphous-carbon film is indented by a sp^3 bonded tip. The dark gray spheres are the carbon atoms in the tip, the light gray spheres are the carbon atoms in the film, the white spheres represent surface hydrogen atoms, and the black spheres represent tip hydrogen atoms. (a) Time=0.0 ps, (b) time=8.0 ps, (c) time=14.9 ps.

different local densities.[34] Therefore the response of the nonuniformly distributed carbon clusters will be more complicated than the classical case. The observed compressive stresses (average value of 120 GPa in the vicinity of the indentor) do not extend to the diamond substrate. After the tip is withdrawn, only about 1.5% of the atoms in the *a*-C:H film have larger compressive stresses than they had prior to indentation, and less than 0.3% have larger shear stresses. The average compressive stress is about 6.0 GPa and the average shear stress is about 4.6 GPa.

To ascertain the extent of rearrangement, the bonding character of the film was examined after indentation. The hybridization of the indented *a*-C:H film is: 20% of the carbon atoms are sp^3 hybridized, 59% are sp^2 hybridized, 1% of the carbon atoms have only two nearest neighbors, and 0.1% of the carbon atoms have five nearest neighbors. This indicates that no significant rearrangement of the *a*-C:H film took place during indentation. After the tip is withdrawn, no depression is left on the surface of the *a*-C:H film [Fig. 3(c)]; therefore the indentation is considered to be elastic.

The loading portion of the force-distance curve is again linear (Fig. 4) and is related to the reduced modulus of the tip and film. Linear regression (inset Fig. 4) yields a slope of 18.4 nN/Å. Using Eq. (1), a value of 153 GPa is obtained for

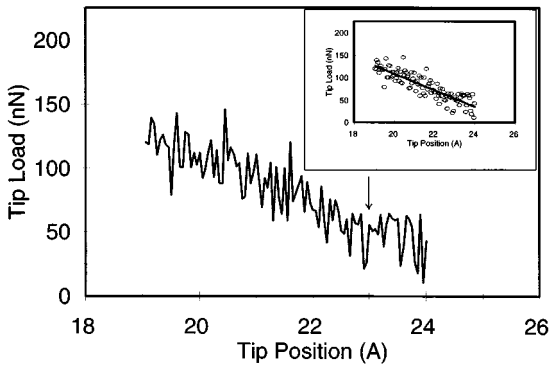

FIG. 4. Force on the tip vs distance of the tip for the indentation of the amorphous-carbon thin film. Only the loading portion of the curve is shown. The arrow indicates the point where the tip first touches the film. The inset shows the line of best fit to the data.

the reduced modulus. From Eq. (2), the modulus of the *a*-C:H film is estimated to be 243 GPa. If one assumes the tip has the same modulus as diamond, Eq. (2) would give a value of 157 GPa for the modulus of the *a*-C:H film. Hence determining the relative modulus of the tip in the C(111):H indentation is important in calculating the modulus of the *a*-C:H film.

Experimental values for the elastic moduli of amorphous-carbon films vary depending on deposition conditions, growth technique, and the sp^3 to sp^2 ratio. Films made by laser plasma discharge with an sp^3 to sp^2 ratio of 3:1 (75% diamondlike) have a Young's modulus of 369 GPa.[35] Lowering the percent diamondlike character of the film reduces the modulus. Films made by ion beam assisted deposition have moduli between 100 and 260 GPa for films with 0%–16% diamondlike character.[36] Sputtered, amorphous-carbon films have a modulus of approximately 140 GPa.[37] Amorphous-carbon films (that contain hydrogen) deposited by rf plasma are found to have moduli between 120 and 140 GPa.[38] The value of the modulus obtained here is thus within the expected range for *a*-C:H films.

IV. SUMMARY

Simulations have been performed that model the nanometer-scale indentation of *a*-C:H with a sp^3 bonded tip. The simulations have revealed important atomic-scale mechanisms that occur during indentation, such as the twist and shear deformation modes of the tip. We have also examined the effects of tip penetration on the arrangement of the carbon atoms within the thin film. Little change in the hybridization of the carbon atoms or the randomly distributed compressive and shear (von Mises) stresses within the film are observed after indentation.

Finally, the simulations have allowed us to quantitatively determine the modulus of a thin amorphous-carbon film, which is found to be much softer than bulk diamond. The calculated value of 243 GPa shows good agreement with experiment. Hence, simulations of nanometer-scale indents could be one way of studying the mechanical properties of films too thin to indent experimentally. In addition, the modulus of the tip was determined through an elastic indentation against diamond (111) to have a modulus of 357 GPa, which is significantly different from the modulus of diamond.

In short, the atomistic simulations of the nanometer-scale indentation of a surface and a thin film have provided qualitative insight into the mechanical deformation processes which take place during indentation, and quantitative predictions that compare well with experimental data.

ACKNOWLEDGMENTS

This work was supported by the Office of Naval Research (ONR) through the U.S. Naval Academy (No. N00014-96-WR-20008), the Naval Research Laboratory (No. N00014-95-WX-20120), the University of Kentucky (No. N00014-95-1-1183), and North Carolina State University (No. N00014-95-1-0270). S.B.S. and D.W.B. gratefully acknowl-

edge an Oak Ridge Associated Universities Junior Faculty Enhancement Award and a National Science Foundation CAREER development Grant No. DMR96-32525, respectively. The authors also thank Frederick H. Streitz, James J. C. Barrett, Steven M. Hues, and Sean Corcoran for many helpful discussions. Some of the figures were generated with the program Xmol (Xmol version 1.3.1, Minnesota Computer Center, Inc., Minneapolis, MN, 1993).

[1]*Nanomaterials: Synthesis, Properties and Applications*, edited by A. S. Edelstein and R. C. Commarata (Institute of Physics, London, 1996).
[2]G. Binnig, C. F. Quate, and Ch. Gerber, Phys. Rev. Lett. **56**, 930 (1986).
[3]S. Gould, O. Marti, B. Drake, L. Hellemans, C. E. Bracker, P. K. Hansma, N. L. Keder, M. M. Eddy, and G. D. Stucky, Nature **332**, 332 (1988).
[4]C. M. Mate, G. M. McCelland, R. Erlandsson, and S. Chiang, Phys. Rev. Lett. **59**, 1942 (1987).
[5]R. Erlandsson, G. Hadziloannou, C. M. Mate, G. M. McClelland, and S. Chiang, J. Chem. Phys. **89**, 5190 (1988).
[6]N. A. Burnham and R. J. Colton, J. Vac. Sci. Technol. A **7**, 2906 (1989).
[7]G. J. Germann, S. R. Cohen, G. Neubauer, G. M. McClelland, H. Seki, and D. Coulman, J. Appl. Phys. **73**, 163 (1993).
[8]E. Meyer, R. Overney, D. Brodbeck, L. Howald, R. Luthi, J. Frommer, and H.-J. Guntherodt, Phys. Rev. Lett. **69**, 1777 (1992).
[9]J. Ruan and B. Bhushan, J. Appl. Phys. **76**, 5022 (1994).
[10]J. Hu, X-D. Xiao, D. F. Ogletree, and M. Salmerson, Surf. Sci. **327**, 358 (1995).
[11]S. Fujisawa, E. Kishi, Y. Suguhiro, and S. Morita, Phys. Rev. B **51**, 7849 (1995).
[12]S. G. Corcoran, S. M. Hues, R. J. Colton, D. M. Schaefer, C. F. Draper, G. F. Meyers, B. M. DeKoven, and S. C. Webb, J. Mater. Res. (to be published).
[13]C. M. Mate, M. R. Lorenz, and V. J. Novotny, J. Chem. Phys. **90**, 7550 (1989).
[14]U. Landman, W. D. Luedtke, N. A. Burnham, and R. J. Colton, Science **248**, 454 (1990).
[15]J. A. Harrison and D. W. Brenner in *The Handbook of Micro/Nanotribology*, edited by B. Bhushan (Chemical Rubber, Boca Raton, FL, 1995), and references therein.
[16]J. A. Harrison, C. T. White, R. J. Colton, and D. W. Brenner, Surf. Sci. **271**, 57 (1992); J. A. Harrison, R. J. Colton, C. T. White, and D. W. Brenner, Mater. Res. Soc. Symp. Proc. **239**, 573 (1992).
[17]J. N. Glosli, M. R. Philpott, and J. Belak, Mater. Res. Soc. Symp. Proc. **383**, 431 (1995).
[18]D. W. Brenner, S. B. Sinnott, O. A. Shenderova, and J. A. Harrison (unpublished).
[19]D. W. Brenner, Phys. Rev. B **42**, 9458 (1990); D. W. Brenner, J. A. Harrison, C. T. White, and R. J. Colton, Thin Solid Films **206**, 220 (1991).
[20]C. W. Gear, *Numerical Initial Value Problems in Ordinary Differential Equations* (Prentice-Hall, Englewood Cliffs, NJ, 1971).
[21]M. H. Grimsditch and A. K. Ramdas, Phys. Rev. B **11**, 3139 (1975).
[22]J. L. Warren, J. Yarnell, G. Dolling, and R. A. Cowley, Phys. Rev. **158**, 805 (1967).
[23]S. B. Sinnott, R. J. Colton, C. T. White, and D. W. Brenner, Surf. Sci. Lett. **316**, L1055 (1994).
[24]J. N. Glosli, J. Belak, and M. R. Philpott, Mater. Res. Soc. Symp. Proc. **356**, 749 (1995).
[25]S. J. Bull, Diam. Relat. Mater. **4**, 827 (1995).
[26]W. Wanlu, J. Kejun, G. Jinying, and L. Aimin, Thin Solid Films **215**, 174 (1992).
[27]L. Abello, G. Lucazeau, B. Andre, and Th. Priem, Diam. Relat. Mater. **1**, 512 (1992).
[28]S. A. Adelmen, Adv. Chem. Phys. **44**, 143 (1980); S. A. Adelmen and J. D. Doll, J. Chem. Phys. **64**, 2375 (1976).
[29]I. N. Sneddon, Int. J. Eng. Sci. **3**, 41 (1965).
[30]The commercial plotting package QUATTRO PRO (version 6.1) was used to perform the linear regression.
[31]D. W. Brenner, S. B. Sinnott, J. A. Harrison, and O. A. Shenderova, Nanotechnology **7**, 1 (1996).
[32]G. E. Henein and J. E. Hillard, J. Appl. Phys. **54**, 728 (1983).
[33]Assuming a reduced modulus of 279 GPa, modulus of the diamond (111) substrate of 1347 GPa, and Poisson's ratio for diamond of 0.10 for both the tip and the substrate.
[34]D. Srolovite, K. Maeda, V. Vitek, and T. Egami, Philos. Mag. A **44**, 847 (1981).
[35]F. Davanloo, T. J. Lee, D. R. Jander, H. Park, J. H. You, and C. B. Collins, J. Appl. Phys. **71**, 1446 (1992).
[36]F. Rossi, B. Andre, A. Van Veen, P. E. Mijnarends, H. Schut, W. Gissler, J. Haupt, G. Lucazeau, and L. Abello, J. Appl. Phys. **75**, 3121 (1994).
[37]J. Robertson, Surf. Coat. Technol. **50**, 185 (1992).
[38]E. H. A. Dekempeneer, R. Jacobs, J. Smeets, J. Meneve, L. Eersels, B. Blanpain, J. Roos, and D. J. Oostra, Thin Solid Films **217**, 56 (1992).